Molecular Pharmacology Fast Forward. Published on February 23, 2009 as doi:10.1124/mol.108.054494

MOL # 54494

Nicotine Normalizes Intracellular Subunit Stoichiometry of Nicotinic Receptors Carrying Mutations linked to Autosomal Dominant Nocturnal Frontal Lobe Epilepsy

Cagdas D. Son, Fraser J. Moss, Bruce N. Cohen, Henry A. Lester

Division of Biology, California Institute of Technology, Pasadena, California 91125

Molecular Pharmacology Fast Forward. Published on February 23, 2009 as DOI: 10.1124/mol.108.054494
This article has not been copyedited and formatted. The final version may differ from this version.

MOL # 54494

Running Title Page: *ADNFLE: a disease of nAChR stoichiometry*

Corresponding author: Henry A. Lester,

Division of Biology, MC 156-29,

California Institute of Technology,

Pasadena, California 91125, USA.

Tel. (626) 395-4946; Fax. (626) 564-8709

e-mail: lester@caltech.edu

Text pages: 40 when double-spaced

Tables: 1

Figures: 6

References: 48

Words: Abstract: 248

Introduction: 645

Discussion: 1452

ABBRIVIATIONS: ADNFLE, Autosomal dominant nocturnal frontal lobe epilepsy; nAChR, neuronal nicotinic acetylcholine receptors; FRET, Förster resonance energy transfer; CFP and YFP, cyan and yellow fluorescent protein; NFLE, Nocturnal frontal lobe epilepsy; NREM, non-rapid eye movement; EEG, electroencephalogram; ACh, acetylcholine; FIR, fluorescence intensity ratios; DRAP, donor recovery after acceptor photobleaching; DMEM, Dulbecco's Modified Eagle Medium; SPT, spectral bleedthrough.

Molecular Pharmacology Fast Forward. Published on February 23, 2009 as DOI: 10.1124/mol.108.054494
This article has not been copyedited and formatted. The final version may differ from this version.

Abstract

Autosomal dominant nocturnal frontal lobe epilepsy (ADNFLE) is linked with high penetrance to several distinct nicotinic receptor (nAChR) mutations. We studied $(\alpha4)_3(\beta2)_2$ vs $(\alpha4)_2(\beta2)_3$ subunit stoichiometry for five channel-lining M2 domain mutations: S247F, S252L, 776ins3 in α4, and V287L, V287M in β2. α4 and β2 subunits were constructed with all possible combinations of mutant and wild type (WT) M2 regions, of cyan and yellow fluorescent protein (CFP, YFP), and of fluorescent and non-fluorescent M3-M4 loops. Sixteen fluorescent subunit combinations were expressed in N2a cells. Förster resonance energy transfer (FRET) was analyzed by donor recovery after acceptor photobleaching and by pixel-by-pixel sensitized emission, with confirmation by fluorescence intensity ratios. Because FRET efficiency is much greater for adjacent than for non-adjacent subunits and the α4 and β2 subunits occupy specific positions in nAChR pentamers, observed FRET efficiencies from $(\alpha4)_3(\beta2)_2$ carrying fluorescent α4 subunits were significantly higher than for $(\alpha4)_2(\beta2)_3$; the converse was found for fluorescent β2 subunits. All tested ADNFLE mutants produced 10-20% increments in the percentage of intracellular $(\alpha4)_3(\beta2)_2$ receptors compared to wild type (WT) subunits. In contrast, 24-48 h nicotine (1 μM) exposure increased the proportion of $(\alpha4)_2(\beta2)_3$ in WT receptors and also returned subunit stoichiometry to WT levels for α4S248F and β2V287L nAChRs. These observations may be relevant to the decreased seizure frequency in ADNFLE patients who use tobacco products or nicotine patches. Fluorescence-based investigations of nAChR subunit stoichiometry may provide efficient drug discovery methods for nicotine addiction or for other disorders that result from dysregulated nAChRs.

Molecular Pharmacology Fast Forward. Published on February 23, 2009 as DOI: 10.1124/mol.108.054494
This article has not been copyedited and formatted. The final version may differ from this version.

Introduction

Nocturnal frontal lobe epilepsy (NFLE) is marked by seizures that include rhythmic and repetitive limb movements, rapid uncoordinated movements, dystonic posturing, complex motor activities such as sleep walking and pelvic thrusting, and the elevation of the trunk and head with ictal fear and vocalization. NFLE seizures occur primarily during phase 2 of non-rapid eye movement (NREM) sleep. They rarely progress to tonic-clonic convulsions or status epilepticus. There are often uncertain distinctions between NFLE and paroxysmal sleep disorders. The "frontal" description arises from ictal EEG data, where available, and seizure semiology origin (Combi et al., 2004; Derry et al., 2006; Herman et al., 2001; Provini et al., 1999; Ryvlin et al., 2006).

Autosomal dominant NFLE (ADNFLE) (Scheffer et al., 1995) is linked, with high penetrance, to at least six distinct nAChR mutations in α4β2 neuronal nicotinic acetylcholine receptors (nAChRs) (Combi et al., 2004; Oldani et al., 1998; Steinlein et al., 1997; Wimmer et al., 2008). Three mutations are in the channel-lining M2 domain of the α4 subunit (S247F=S6'F in the commonly used M2 domain renumbering for Cys-loop receptors, S252L=S10'L and 776ins3, after the 17' position), while two mutations are at the M2 domain of the β2 subunit (V287L and V287M at the 22' position). How the ADNFLE-linked mutations cause seizures, the epileptic focus of ADNFLE seizures, and other basic pathophysiological aspects remain unresolved.

Simple loss of α4β2 receptor function does not appear to cause ADNFLE. Knockout (KO) mice with genetic deletions of the α4 or β2 subunit do not display spontaneous seizures or any nicotine-induced phenotype resembling ADNFLE seizures (Teper et al., 2007; Wong et al., 2002) (personal communication, Dr. Marina Picciotto). One hypothesis suggests that ADNFLE mutations

Molecular Pharmacology Fast Forward. Published on February 23, 2009 as DOI: 10.1124/mol.108.054494
This article has not been copyedited and formatted. The final version may differ from this version.

initiate seizures by increasing the sensitivity of α4β2 nicotinic receptors to the endogenous agonist acetylcholine (ACh) (Bertrand et al., 2002). Our own work (Figl et al., 1998; Rodrigues-Pinguet et al., 2003; Rodrigues-Pinguet et al., 2005) and that of others (Steinlein et al., 1997) shows that reduced allosteric Ca^{2+} potentiation of the α4β2 ACh response is another common feature of ADNFLE mutations.

A more subtle pathophysiological suggestion arises from the observations that α4β2 nAChRs exists at least in two different stoichiometries. Although the stoichiometry of human α4β2 nAChRs in neurons has not yet been elucidated, in mouse brain preparations there are biphasic agonist concentration-response curves for stimulation of putative α4β2 nAChR function (Fonck et al., 2005; Fonck et al., 2003). Similarly, α4 and β2 nAChR subunits that are expressed heterologously in mammalian cell lines (Kuryatov et al., 2005; Nelson et al., 2003; Vallejo et al., 2005) or *Xenopus* oocytes (Zwart et al., 2006) assemble into a mixture of receptors with two distinct agonist sensitivities. The dominant stoichiometry in these heterologous systems is often the low-sensitivity $(\alpha4)_3(\beta2)_2$ nAChR (Kuryatov et al., 2005; Moroni et al., 2006; Nelson et al., 2003). Most investigations of heterologously expressed ADNFLE mutants reveal left-shifted dose-response relations, so it has been natural to suspect that this arises from altered subunit stoichiometry.

Nicotine and tobacco use decreases the frequency of ADNFLE seizures (Brodtkorb and Picard, 2006; Willoughby et al., 2003). α4β2 receptors may be the primary nAChR subtype affected by nicotine concentrations (100 - 500 nM) found in the blood of smokers (Benowitz et al., 1982). Chronic exposure to nicotine initiates a cascade of events such as activation and desensitization of nAChRs, induction of long-term potentiation and depression at glutamatergic synapses (Mansvelder and McGehee, 2000; Partridge et al., 2002), behavioral tolerance,

Molecular Pharmacology Fast Forward. Published on February 23, 2009 as DOI: 10.1124/mol.108.054494
This article has not been copyedited and formatted. The final version may differ from this version.

dependence and withdrawal. Chronic exposure to nicotine also causes a shift in nAChR subunit stoichiometry in heterologous expression systems (Nelson et al., 2003). To understand whether the nAChR subunit stoichiometry is altered in ADNFLE, and how nicotine might have an effect on seizure suppression, we analyzed the effects of each mutation on α4β2 nAChR subunit stoichiometry. We also analyzed effects of nicotine. The primary tools were Förster resonance energy transfer (FRET) and fluorescence intensity ratios (FIR).

Molecular Pharmacology Fast Forward. Published on February 23, 2009 as DOI: 10.1124/mol.108.054494
This article has not been copyedited and formatted. The final version may differ from this version.

Materials and Methods

Materials

pEYFP-C1 and pECFP-C1 vectors were purchased from Clontech (Mountain View, CA). PfuTurbo C_x Hotstart polymerase and the Quickchange II XL site-directed mutagenesis kit were purchased from Stratagene (La Jolla, CA). The mouse neuroblastoma 2a (N2a; CCL-131) was obtained from ATCC (Manassas, VA). The pcDNA3.1(+) expression vector, fetal bovine serum (FBS), Lipofectamine and Plus reagents were purchased from Invitrogen (Carlsbad, CA). Penicillin/Streptomycin 100X and sodium pyruvate 100× solutions were purchased from Mediatech (Herndon, VA). Culture dishes (35 mm, with 14 mm No. 0 glass coverslip microwells) were purchased from Mattek (Ashland, MA). Other tissue-culture plasticware was purchased from Greiner Bio-One (Monroe, CA). Acetylcholine chloride (ACh), nicotine and all other reagents were purchased from SigmaAldrich (St. Louis, MO).

Molecular Biology

Wild-type mouse α4 and β2 nAChR cDNAs were kindly provided by Jerry Stitzel (University of Michigan, Ann Arbor, MI) and the construction of fluorescent α4YFP, α4CFP and β2YFP, β2CFP nAChR subunits has been described (Nashmi et al., 2003). Fluorescent ADNFLE mutants were generated in QuikChange II XL mutagenesis PCR reactions from the WT α4XFP and β2XFP plasmids using the primer pairs described in Supplementary Table 1. For each construct, the entire open reading frame and its flanking regions were sequenced.

Molecular Pharmacology Fast Forward. Published on February 23, 2009 as DOI: 10.1124/mol.108.054494
This article has not been copyedited and formatted. The final version may differ from this version.

Cell culture and transfections

N2a cells were cultured at 37 °C in 95% air, 5% CO_2 in medium composed of 44.5% DMEM, 44.5% OptiMEM1, 5% FBS, 100 I.U./ml penicillin and 100 µg/ml streptomycin. For all experiments, cells were plated onto poly-*d*-lysine coated 35 mm culture dishes with 14 mm glass bottoms. Transfections were performed using a modification of the manufacturer's Lipofectamine and Plus reagent protocol, resulting in non-saturated expression levels of nAChRs (Imoukhuede et al., 2009). cDNA was diluted in DMEM in one tube to which Plus reagent was subsequently added. The total cDNA in each transfection mix was always 1 µg and the proportion of α4 and β2 cDNAs used in each experiment are stated in the relevant results section. In a second tube, Lipofectamine was diluted in DMEM. The tubes were briefly vortexed and incubated at room temperature for 15 min. The diluted Lipofectamine was subsequently added to the cDNA/Plus reagent dilution and vortexed. The transfection mixes were incubated for a further 15 min at room temperature, while the pre-plated cells were washed once with DMEM to remove residual serum from the culture media and then 800 µl of DMEM added to perform the transfection. Sixteen h after the cells were originally plated, the cDNA/Plus/Lipofectamine mixes (200 µl) were added to the dishes. The transfections were incubated at 37 ° C for 3 h; then 2.5 ml of N2a medium was added. Nicotine at 1 µM final concentration was added to the appropriate dishes (nicotine was replenished with each change of medium). After 16 h the transfection cocktail was replaced by complete N2a medium and again 24 h later.

Confocal Imaging

Live cells grown on 14 mm glass bottomed Mattek 35 mm culture dishes pre-coated with poly-*d*-lysine were washed twice with 37 °C, pH 7.4 extracellular buffer (150 mM NaCl, 4 mM

Molecular Pharmacology Fast Forward. Published on February 23, 2009 as DOI: 10.1124/mol.108.054494
This article has not been copyedited and formatted. The final version may differ from this version.

KCl, 10 mM HEPES, 2 mM $MgCl_2$, 2 mM $CaCl_2$, 10 mM glucose) and observed in the same solution. Imaging was performed at room temperature on an Eclipse C1si laser scanning confocal microscope equipped with a 63×, 1.4 NA VC Plan Apo oil objective and a multi-anode PMT with 32 channels (Nikon Instruments Inc., Melville, NY). Where required, images were linearly unmixed with the EZ-C1 software (Nikon) for the emission spectra of the fluorophores of interest using reference spectra individually compiled for each fluorophore expressed in the same cell type and imaged under identical experimental conditions. Quantification of images was performed using ImageJ version 1.41g.

Donor Recovery after Acceptor Photobleach Förster Resonance Energy Transfer (DRAP-FRET)

N2a cells were visualized at room temperature in extracellular buffer, 48 h after transfection. A series of lambda stack X-Y images were collected with the Eclipse C1si laser scanning confocal microscope. Dequenching of CFP fluorescence during incremental photobleaching of YFP was performed and analyzed as previously described (Drenan et al., 2008; Nashmi et al., 2003). FRET efficiency (E) was calculated:

$$E = 1 - \left(\frac{I_{DA}}{I_D} \right) \qquad \text{(Equation 1)}$$

I_{DA} represents the normalized fluorescence intensity of CFP (100%) in the presence of non-bleached acceptor. I_D represents the normalized fluorescence intensity of CFP following 100% photobleach of the acceptor, YFP. The I_D value was extrapolated from a scatter plot of the percentage increase of CFP versus the percentage decrease of YFP for each cell (Nashmi et al., 2003). This method of determining FRET is used for the data in Figure 2, Figure 3, and Figure 4 below.

Molecular Pharmacology Fast Forward. Published on February 23, 2009 as DOI: 10.1124/mol.108.054494
This article has not been copyedited and formatted. The final version may differ from this version.

Pixel-by-pixel FRET from sensitized acceptor emission

Full emission spectra were acquired in 5 nm bins between 450 nm and 610 nm and linearly unmixed using reference spectra from samples expressing solely the CFP- or YFP-fusion constructs to separate the CFP and YFP signal from each pixel of the spectral images. Transfections of cells expressing only the CFP- or YFP-fusion protein were performed for every imaging session to control for pixel saturation and spectral bleedthrough (SBT). Where appropriate, non-fluorescent subunit cDNAs were included in the transfection to ensure the faithful expression and subcellular localization of the single fluorescent species. Control samples expressing only the CFP-fusion constructs were imaged with the 439.5 nm laser line and unmixed with YFP and CFP spectra. The unmixed YFP images were termed the $FRET_C$ channel, and the fluorescence intensity of each pixel was termed (I_{FRETC}). The CFP images were the "Donor" channel and pixel intensities were described by I_{CFP}. A montage of all the $FRET_C$ channel images and a second montage of all the Donor channel images were assembled and compiled into an image stack called the "Donor SBT stack" in the order $FRET_C$ channel, Donor channel. Two spectral images of each cell expressing only the YFP fusion constructs were acquired, the first excited by the 439.5 nm laser line and the second with the 514 nm laser line. The YFP signal was unmixed from each image. A montage of the unmixed 439.5 nm excited YFP images termed the $FRET_Y$ channel (pixel intensities = I_{FRETY}) was assembled and compiled with a montage of the 514 nm excited YFP images termed the Acceptor channel (pixel intensities = I_{YFP}) and called the Acceptor SBT image stack.

The Donor and Acceptor SBT stacks were processed by the Pix-FRET ImageJ plugin to assess the CFP and YFP bleedthroughs (Feige et al., 2005). The donor SBT ratio (I_{FRETC}/I_{CFP}) was plotted as a function of I_{CFP} to model the CFP SBT (BT_{CFP}) for each pixel in the FRET images. The acceptor SBT ratio (I_{FRETY}/I_{YFP}) was plotted as a function of I_{YFP} to model the YFP bleedthrough

Molecular Pharmacology Fast Forward. Published on February 23, 2009 as DOI: 10.1124/mol.108.054494
This article has not been copyedited and formatted. The final version may differ from this version.

(BT_{YFP}) for each pixel in the FRET images. If linear, the best fit of the bleedthrough plot gave the constants a_{XFP} and b_{XFP} in the equation $BT_{XFP} = a_{XFP} I_{XFP} + b_{XFP}$ (where XFP is either the donor or the acceptor fluorophore). If an exponential, the best fit of the bleedthrough plot gave the constants c_{XFP}, d_{XFP} and e_{XFP} in the equation $BT_{XFP} = c_{XFP} exp(I_{XFP} d_{XFP}) + e_{XFP.}$

Unmixed images for each cell were compiled into stacks of three 16-bit images in the channel order FRET, Donor and Acceptor. From this stack a region of interest was selected to determine the background intensity for all three images in the stack. With the background and SBT corrections set, the net FRET (*nF*) for each pixel was calculated, and the data were output as 32-bit image:

$$nF = I_{FRET} - I_{CFP} BT_{CFP} - I_{YFP} BT_{YFP} . \quad \text{(Equation 2)}$$

FRET efficiency could not be directly determined by Equation 1 from sensitized emission experiments because it is not possible to measure I_D directly from such samples. However, because the sensitized emission of the acceptor is due to the quenching of the donor in the presence of the acceptor, I_D can be determined (Elangovan et al., 2003) by adding the *nF* signal intensity to the intensity of the donor in the presence of acceptor I_{DA}. Substituting $I_D = I_{DA} + nF$ into Equation 1, one has:

$$E = 1 - \left(\frac{I_{DA}}{I_{DA} + nF} \right), \quad \text{(Equation 3)}$$

This method for measuring FRET is employed for the data in Figure 5 and Figure 6 below.

Molecular Pharmacology Fast Forward. Published on February 23, 2009 as DOI: 10.1124/mol.108.054494
This article has not been copyedited and formatted. The final version may differ from this version.

Results

FRET efficiencies reflect stoichiometry

The calculations and analyses presented in the Appendix, and summarized by Figure 1 show that when (a) only the α4 subunits are fluorescently tagged with a 1:1 molar ratio of CFP and YFP, and (b) the $(\alpha4)_3(\beta2)_2$ receptor stoichiometry predominates, one expects robust FRET. Upon a shift towards the $(\alpha4)_2(\beta2)_3$ stoichiometry, one expects a lower FRET efficiency. These expected differences in FRET arise because, in a pentamer containing three α4 subunits, two are adjacent. Because the FRET efficiency approaches a $1/R^6$ dependence as fluorophores are separated, our assumptions lead to a much higher FRET efficiency in this case. Similarly, (a) when only the β2 subunits are fluorescently tagged with a 1:1 molar ratio of CFP and YFP, and (b) when the $(\alpha4)_2(\beta2)_3$ receptor stoichiometry predominates, one expects a higher FRET efficiency.

Cells often produce a mixture of these $(\alpha4)_2(\beta2)_3$ and $(\alpha4)_3(\beta2)_2$ receptors (Buisson and Bertrand, 2001; Nashmi et al., 2003; Nelson et al., 2003), although they can be manipulated to express a nearly pure population of one or the other (Briggs et al., 2006; Nelson et al., 2003). We have optimized an N2a cell expression system to produce controlled, nonsaturated expression of membrane proteins, suitable for fluorescence studies (Drenan et al., 2008; Imoukhuede et al., 2009). We transfected N2a cells with various ratios of subunit cDNA, to force the receptor population towards a mostly $(\alpha4)_3(\beta2)_2$ or $(\alpha4)_2(\beta2)_3$ stoichiometry (Nelson et al., 2003). As typically found for nAChRs, there was little or no membrane-localized fluorescence at the cell periphery in any of the images of this study; therefore most of the fluorescence arises from intracellular receptors.

To study FRET, we intentionally bleached the YFP fluorophore while monitoring fluorescence from both the YFP and CFP fluorophores. Changes in fluorescence intensity versus

Molecular Pharmacology Fast Forward. Published on February 23, 2009 as DOI: 10.1124/mol.108.054494
This article has not been copyedited and formatted. The final version may differ from this version.

time were plotted (Figure 2B), and FRET efficiency was calculated as described in Methods (Figure 2C, D, E). Measured FRET efficiencies ranged from 5 to 18 percent for various transfections with forced stoichiometries. As expected, we observed a monotonic increase in FRET when the fluorophores were attached to the α4 subunit and the mole fraction of α4 cDNA was increased, shifting the stoichiometry toward $(\alpha4)_3(\beta2)_2$ (Figure 2D). Similarly, higher FRET efficiencies were observed when the fluorophores are attached to the β2 subunit and the stoichiometry was shifted toward $(\alpha4)_2(\beta2)_3$ population.

We correlated these measurements with the calculated values, assuming 52 Å as the shortest distance *a* between two fluorophores, using the linear relation summarized in Figure 1D. Results showed that when the N2a cells are transfected with 4:1 cDNA ratio of α4:β2, ~90% of the assembled receptors have the $(\alpha4)_3(\beta2)_2$ stoichiometry. Increasing the mole fraction of the β2 cDNA in the transfection mixture increased the $(\alpha4)_2(\beta2)_3$ form, as expected. Interestingly, transfection with 1:1 cDNA ratio resulted in 60 - 70% $(\alpha4)_3(\beta2)_2$; similar results were previously reported using biochemical assays (Nelson et al., 2003). Importantly, these results are also confirmed by an independent series of measurements that use FIR ((Supplementary) Figure 7). These results confirmed that qualitatively, and to some extent quantitatively, higher FRET is observed when there are three rather than two fluorophore-labelled subunits of a single subtype in $(\alpha4)_n(\beta2)_{5-n}$ receptors.

ADNFLE mutations bias stoichiometry toward $(\alpha4)_3(\beta2)_2$: DRAP assays

In one set of experiments, we analyzed DRAP FRET efficiency values from N2a cells transfected with non-fluorescent ADNFLE mutants plus fluorescently tagged complementary wild-type subunits (Figure 3A, B). There were two subsets of these experiments. One used α4 ADNFLE subunits plus fluorescent β2 subunits (denoted β2XFP in Figure 3A, B); the other used β2

Molecular Pharmacology Fast Forward. Published on February 23, 2009 as DOI: 10.1124/mol.108.054494
This article has not been copyedited and formatted. The final version may differ from this version.

ADNFLE subunits plus fluorescent α4 subunits (denoted α4XFP in Figure 3A, B). We carried out 1:4 (Figure 3A) and 1:1 cDNA (Figure 3B) transfection ratios for the two nAChR subunits α4 and β2, respectively. (We chose the 1:4 ratio because, as shown below, the ADNFLE mutations seem to favor nAChRs containing more α4 than β2 subunits; and it was important to know whether merely changing the cDNA ratios could reverse this effect). In nearly all cases, FRET values differed significantly from the values for the corresponding fluorescently labeled wild type subunits. The α4 mutants tested (776ins3, S248F and S252L) showed significantly lower FRET efficiencies compared to the α4β2XFP control. This decrease in FRET efficiency suggested an increased $(\alpha4)_3(\beta2)_2$ receptor population versus the WT subunits. On the other hand the two β2 subunit ADNFLE mutants showed a significant increase in FRET efficiency compared to the α4XFPβ2 control. These results also suggest an increased $(\alpha4)_3(\beta2)_2$ receptor population versus the control cells. All five of the 1:4 cDNA transfection pairs (Figure 3A), and all five of the 1:1 cDNA transfection pairs Figure 3B, displayed a significant shift in subunit stoichiometry toward the $(\alpha4)_3(\beta2)_2$ configuration.

In a second set of experiments, we analyzed FRET efficiency values from N2a cells transfected with subunits that contained both ADNFLE mutations and XFP labels (Figure 3C, D). The complementary subunits were WT. These experiments were performed with the five M2 domain ADNFLE mutations studied in the experiments described above. Again, there were two subsets of these experiments. One used α4 ADNFLE fluorescent subunits (denoted α4XFP in Figure 3C, D) plus non-fluorescent β2 subunits; the other used β2 ADNFLE fluorescent subunits (denoted β2XFP in Figure 3C, D) plus non-fluorescent α4 subunits. We carried out 1:4 cDNA (Figure 3C) and 1:1 cDNA (Figure 3D) transfection ratios for the α4 and β2 subunits, respectively. In four of five cases for both transfection ratios, the change in the FRET efficiency indicated a shift towards the $(\alpha4)_3(\beta2)_2$ receptor population.

Molecular Pharmacology Fast Forward. Published on February 23, 2009 as DOI: 10.1124/mol.108.054494
This article has not been copyedited and formatted. The final version may differ from this version.

This set of DRAP FRET experiments shows that, under 18 of 20 conditions, the ADNFLE mutations significantly ($p < 0.05$) shift the stoichiometry of α4β2 receptor population toward the $(\alpha4)_3(\beta2)_2$ stoichiometry. This major result is consistent across several experimental conditions. The ADNFLE mutation is in either the α4 or the β2 subunit; the fluorescent groups are in either the mutant or non-mutant subunit; the fluorescent control groups are in either the α4 or the β2 subunits; the subunit cDNAs are transfected at roughly equal levels or with excess β2 cDNA. Thus, we can rule out effects on expression or assembly caused by the subunit carrying the mutation, by the type of fluorescent moiety (YFP vs CFP), or by its presence in a particular subunit.

Nicotine counteracts the bias toward $(\alpha4)_3(\beta2)_2$ of ADNFLE receptors

Effects of chronic nicotine on nAChR subunit stoichiometry have been studied previously by several groups (Moroni et al., 2006; Nelson et al., 2003). These studies showed that exposure to nicotine preferentially upregulates a high-sensitivity receptor population. For WT receptors, this population is usually assigned to the $(\alpha4)_2(\beta2)_3$ stoichiometry. We asked whether incubation with nicotine shifts ADNFLE receptors toward the $(\alpha4)_2(\beta2)_3$ stoichiometry, despite the bias toward the opposite stoichiometry.

We first describe experiments with WT, fluorescent receptors (Figure 4A). Incubation in nicotine produced a significant decrease or increase in FRET efficiency when the XFP probes were in the α4 or β2 subunits, respectively. This indicates that, as expected, incubation in nicotine shifts the receptor population toward the $(\alpha4)_2(\beta2)_3$ stoichiometry. Our studies with fluorescence intensity ratios of subunit stoichiometry (Table 1 and Supplementary Material) agree with these findings.

Molecular Pharmacology Fast Forward. Published on February 23, 2009 as DOI: 10.1124/mol.108.054494
This article has not been copyedited and formatted. The final version may differ from this version.

We next describe analogous experiments with an ADFLE mutation, β2 V287L (Figure 4B). In cells transfected with α4 and β2 V287L XFP subunits, FRET efficiency was significantly higher after incubation in nicotine compared to control cells that were not exposed to nicotine. Likewise, cells transfected with α4XFP β2 V287L and treated with nicotine showed lower FRET efficiency than unexposed cells. This result suggests a shift in stoichiometry towards $(\alpha4)_2(\beta2)_3$ in the presence of nicotine, partially or completely counteracting the shift produced by the ADNFLE mutant alone toward the $(\alpha4)_3(\beta2)_2$ population. The observed change in FRET efficiency in the presence of nicotine from cells transfected with α4XFP and β2 V287L subunit was sufficient to bring the average values back to wild type levels; this indicates that cells carrying an ADNFLE mutation in the presence of nicotine had similar subunit stoichiometry to the wild type controls. The nicotine-induced shift was greater when the β2 V287L subunits were tagged with fluorescent proteins. In these cases the effect of nicotine was dominant and the average FRET efficiencies obtained from cells transfected with α4β2XFP and α4β2(V287L)XFP in the presence of nicotine did not differ significantly.

ADNFLE mutations bias toward $(\alpha4)_3(\beta2)_2$: sensitized emission assays

We also analyzed the ADNFLE mutations β2 V287L and α4 S248F, and the effects of chronic nicotine, using pixel-resolved sensitized emission FRET measurements as described in Methods (Figure 5 and Figure 6). Sensitized emission measurements have the advantages of (1) speed, requiring only a few s, (2) greater resolution, allowing pixel-by-pixel measurements, and (3) nondestructive readout, allowing for repeated measurement on a given cell. However sensitized emission measurements require greater attention to corrections for spectral unmixing and bleedthrough. Results obtained with the sensitized emission method agreed well with our DRAP results under the same conditions. Cells transfected with fluorescently tagged β2 V287L ADNFLE

Molecular Pharmacology Fast Forward. Published on February 23, 2009 as DOI: 10.1124/mol.108.054494
This article has not been copyedited and formatted. The final version may differ from this version.

mutant subunits showed a significant 1.3-fold decrease in the mean FRET efficiency vs fluorescent non-ADNFLE subunits (Figure 5A, B, G). On the other hand we detected a significant 1.4-fold higher mean FRET efficiency from cells transfected with α4XFP and β2V287L compared to the control cells transfected with WT subunits (Figure 5D, E, G). Both of these results imply a shift toward the $(\alpha4)_3(\beta2)_2$ stoichiometry.

Upon incubation of these cells with 1 μM nicotine for 48 hr, the mean β2 inter-subunit FRET efficiency increased, to a level even higher than the control cells transfected with non-mutant fluorescent subunits (Figure 5C, G). Exposure to 1 μM nicotine for 48 h resulted in a decrease in the observed α4 intersubunit FRET efficiency, in this case completely back to WT levels (Figure 5F, G). Both of these results showed that incubation in nicotine produces at least a reverse in the shifted stoichiometry that results from the ADNFLE mutation.

We also asked whether nicotine shifted the stoichiometry toward $(\alpha4)_2(\beta2)_3$ for the α4 S248F mutation (Figure 6). Experiments were performed with α4 subunits carrying both the S248F mutation and XFP moieties. We found that incubation in nicotine (1 μM, 48 h) shifted the population toward the $(\alpha4)_2(\beta2)_3$ stoichiometry. Thus for the two ADNFLE mutations tested (one in the α4 subunit, one in the β2 subunit), nicotine appears to partially or completely counteract the mutation-induced bias toward the $(\alpha4)_3(\beta2)_2$ stoichiometry.

Fluorescence Intensity Ratios (FIR) agree with FRET measurements

We have also employed a fluorescence intensity ratio (FIR) analysis (Staruschenko et al., 2005) to determine the stoichiometry of α4β2 nAChRs using the same transfection conditions studied in the previous sections. Because the FIR measurements have not been extended to ADNFLE mutations, the method and data are presented briefly here and more fully in

Molecular Pharmacology Fast Forward. Published on February 23, 2009 as DOI: 10.1124/mol.108.054494
This article has not been copyedited and formatted. The final version may differ from this version.

Supplementary material, including (Supplementary) Figure 7. Summarizing the FIR procedure, we conducted two parallel experiments under identical conditions: α4CFP-β2YFP and α4YFP-β2CFP. These fluorescence data allow one to eliminate the differences in the efficiency of the optical systems for the two fluorophores used in these experiments. Thus, we acquired measurements of the actual ratio between α4 and β2 subunits. The data confirmed that changing the ratio of α4 to β2 cDNA governs the ratio of expressed subunits in assembled receptors; and the measured subunit ratios agreed acceptably with the measurements from FRET (see Table 1 below). In other assays, we also detect that nicotine incubation produces the expected increase in the fraction of $(\alpha4)_2(\beta2)_3$ receptors (see Table 1 below).

Overall summary of stoichiometric differences produced by ADNFLE mutations and by nicotine

We summarize the data on comparative stoichiometry from DRAP-FRET, pixel-based FRET, and FIR measurements exemplified in the figures. These data were gathered for the various subunit transfection ratios, various mutants, and various labeling strategies and were analyzed by the relation in Figure 1D or by supplementary Equations 12 and 13, as appropriate. In each experiment, ADNFLE and WT receptors were compared. The percentage of $(\alpha4)_3(\beta2)_2$ receptors is 1.2 times as great for ADNFLE receptors as for WT receptors (at least 12 experiments); the ratio was > 1 in all experiments.

We also summarize the effects of nicotine; in each case, the experiment compared incubation in nicotine vs saline. The percentage of $(\alpha4)_3(\beta2)_2$ ADNFLE receptors is 0.8 times as great after nicotine incubation as after saline incubation (at least five experiments; the ratio was < 1 in all cases).

Molecular Pharmacology Fast Forward. Published on February 23, 2009 as DOI: 10.1124/mol.108.054494
This article has not been copyedited and formatted. The final version may differ from this version.

Discussion

This study's most important conclusions are that ADNFLE may arise from defective regulation of nAChR subunit stoichiometry in an intracellular compartment(s), and that nicotine exposure reverses this defective stoichiometry. The internal consistency of the experiments rules out several alternative explanations. The bias toward $(\alpha4)_3(\beta2)_2$ is measured (a) when fluorescent groups are in either the mutant or non-mutant subunit; (b) for all three known α4 subunit M2 domain ADNFLE mutations as well as for the two known β2 subunit M2 domain mutations; (c) whether the subunit cDNAs are transfected at roughly equal levels or with excess β2 cDNA. The conclusions are supported by two substantially different FRET measurements (DRAP and sensitized emission), and FIR measurements also confirm the dependence of stoichiometry on transfection ratio. Thus, we have confidence that the conclusions do not arise from variations in expression or assembly caused by the fluorescent moiety, by YFP vs CFP, etc. Changes observed in all five cases show that the ADNFLE mutations produce an increment of 10-20% in the percentage of receptors with the $(\alpha4)_3(\beta2)_2$ stoichiometry.

ADNFLE: a disease of nAChR stoichiometry

As noted in the Introduction, the α4β2 nAChRs exist at least in two different stoichiometries, and it has been suggested that left-shifted dose-response relations arise because ADNFLE receptors have altered subunit stoichiometry. The present data strongly support this suggestion. We have used the terms high- and low-sensitivity to refer only to WT receptors, because it is possible that the higher sensitivity stoichiometry for ADNFLE receptors is $(\alpha4)_3(\beta2)_2$. The $(\alpha4)_3(\beta2)_2$ stoichiometry is the more sensitive form of the α4L9'T-β2 receptor (Moroni et al., 2006); and our unpublished data lead to the same conclusion for the α4L9'S-β2 and α4L9'A-β2

Molecular Pharmacology Fast Forward. Published on February 23, 2009 as DOI: 10.1124/mol.108.054494
This article has not been copyedited and formatted. The final version may differ from this version.

receptors, which produce an ADNFLE-like phenotype in knock-in mice (Fonck et al., 2005; Fonck et al., 2003). If we independently knew the dose-response relations (or at least their relative positions) for the two stoichiometries of ADNFLE mutants, we could employ agonist-induced conductances to infer the relative surface stoichiometry of the ADNFLE mutations. However the ADNFLE mutations probably have more subtle gating effects than the α4L9'T, L9'S, and L9'A mutations, vitiating assumptions about the relative sensitivities; and at present biochemical or fluorescence-based procedures lack the sensitivity to provide this information for the surface membrane compartment.

The internal consistency of the experiments argues against the possibility that our conclusions about altered stoichiometry, and about the effects of nicotine on this stoichiometry, derive artifactually from the presence of partially assembled "dead end" nAChRs (Kuryatov et al., 2005; Kuryatov et al., 2008). Also, the N2a expression system produces considerably lower levels of transfected membrane protein than do HEK293T cells, which produce appreciable numbers of dead-end nAChRs. However we cannot rule out the possibility that partially assembled receptors produce some of the fluorescence.

How subunit dysregulation underlies the pathophysiology of ADNFLE is not known. Despite the left-shifted dose-response relations, in mammalian cells ADNFLE mutations produce rather low maximal ACh sensitivity or surface receptor levels (Kuryatov et al., 2005); and synaptosomes isolated from ADNFLE or ADNFLE-related knock-in mice generally show reduced function and reduced receptor numbers (Fonck et al., 2005; Fonck et al., 2003; Teper et al., 2007)(Jian Xu, Duncan C. Laverty, Carlos Fonck, Michael J. Marks, Gustavo Dziewczapolski, Bruce N. Cohen, Yongling Zhu, Sharon R. Grady, Satchin Panda, Allan C. Collins, Henry A. Lester, and Stephen F. Heinemann, unpublished data). These may be important clues for the

Molecular Pharmacology Fast Forward. Published on February 23, 2009 as DOI: 10.1124/mol.108.054494
This article has not been copyedited and formatted. The final version may differ from this version.

pathophysiology of ADNFLE. Data are beginning to appear about functional effects of auxiliary subunits in nAChRs (Kuryatov et al., 2008), but as noted above, we cannot yet address the important pathophysiological question, whether the altered intracellular stoichiometry of the intracellular receptors leads to similarly altered stoichiometry of surface receptors. Also we still have an incomplete picture of the relation between stoichiometry and surface expression in various cellular regions (dendrites, soma, axons, and axon terminals). Because the seizures occur at night when the endogenous ACh levels are low, the seizures may be initiated by an imbalance between inhibitory and excitatory synaptic transmission (Klaassen et al., 2006; Rodrigues-Pinguet et al., 2005). Perhaps other epilepsies linked to Cys-loop receptors also arise from altered subunit stoichiometry (Wimmer et al., 2008).

Nicotine effects

Chronic agonist or antagonist treatment is often associated with the functional and/or numerical upregulation of α4β2 nAChRs. Therefore it has also been natural to suggest that repeated or chronic exposure to nicotine favors the high-sensitivity $(\alpha4)_2(\beta2)_3$ stoichiometry (Nashmi and Lester, 2007; Nelson et al., 2003; Sallette et al., 2005). The control experiments with WT subunits did extend the previous reports showing that chronic exposure to nicotine results in an upregulation of the $(\alpha4)_2(\beta2)_3$ configuration (Nelson et al., 2003) (FRET: Figure 4A, Figure 5; FIR: Table 1).

The effect of nicotine incubation on the α4β2V287L (Figure 4B, Figure 5G) and α4S248F (Figure 6) nAChRs was similar to the effect on WT: exposure to nicotine favors the $(\alpha4)_2(\beta2)_3$ configuration. We conclude that effects of nicotine are dominant over the effects of the ADNFLE mutation, because nicotine can revert the subunit stoichiometry to nearly WT ratios. This nicotine-induced shift back to the presumably non-pathogenic, WT stoichiometry may help explain how

Molecular Pharmacology Fast Forward. Published on February 23, 2009 as DOI: 10.1124/mol.108.054494
This article has not been copyedited and formatted. The final version may differ from this version.

nicotine patches or smoking suppress seizure phenotype in ADNFLE patients (Brodtkorb and Picard, 2006; Willoughby et al., 2003).

Pharmacological chaperoning by nicotine

Because the present study emphasizes intracellular receptors, it supports recent suggestions that nicotine is an intracellular pharmacological chaperone of WT α4β2 nAChRs (Kuryatov et al., 2005; Nashmi and Lester, 2007; Sallette et al., 2005; Vallejo et al., 2005), stabilizing the $(\alpha4)_2(\beta2)_3$ stoichiometry (Kuryatov et al., 2005) of this multisubunit membrane protein (Balch et al., 2008; Wiseman et al., 2007). Evidently the ADNFLE mutations change the relative stability of the assembled $(\alpha4)_2(\beta2)_3$ and $(\alpha4)_3(\beta2)_2$ conformations, either destabilizing the former or stabilizing the latter. This is slightly surprising, because most of our knowledge about intersubunit contacts lead us to emphasize the N-terminal binding rather than the M2 helices as major determinants of assembly. Nonetheless, the data show that the apparent chaperone effect of nicotine also stabilizes the $(\alpha4)_2(\beta2)_3$ stoichiometry of the ADNFLE mutant subunits, similar to its action on WT subunits. We are interested in conducting FRET experiments to study more details of pharmacological chaperoning by nicotine, including time-resolved measurements and subcellular localization.

Fluorescence-based measurements of subunit stoichiometry

We believe that this study shows the first fluorescence-based distinction between two and three subunits in a pentameric Cys-loop receptor, although the FRET method depends heavily on theories developed for the pentameric MscL channel (Corry and Jayatilaka, 2008; Corry et al., 2006; Corry et al., 2005). Therefore, this report quantitatively extends previous studies of nAChR subunit stoichiometry using fluorescently tagged nAChR subunits, in HEK293T cells (Nashmi et al., 2003), in transfected cultured neurons (Drenan et al., 2008; Khakh et al., 2005; Nashmi et al.,

Molecular Pharmacology Fast Forward. Published on February 23, 2009 as DOI: 10.1124/mol.108.054494
This article has not been copyedited and formatted. The final version may differ from this version.

2003), in knock-in mice (Nashmi and Lester, 2007; Nashmi et al., 2007), and in cultured N2a cells (Drenan et al., 2008). In previous studies, the work of our own laboratory and several others distinguished between 1 and ≥ 2 subunits. FRET theory, combined with the known geometrical and biological constraints in pentameric α4β2 receptor populations, suggested that FRET among α4 subunits, or among β2 subunits, is a sensitive procedure to detect more subtle stoichiometric relations. The explicit theory presented in the Appendix and in Figure 1 (Corry and Jayatilaka, 2008; Corry et al., 2006; Corry et al., 2005) leads to a linear relation between the FRET efficiency and the percent of receptor populations carrying two vs three fluorescently tagged subunits (Figure 1D). The data show that FRET efficiency for $(\alpha4XFP)_3(\beta2)_2$ is indeed significantly higher than for $(\alpha4XFP)_2(\beta2)_3$, and that cells expressing mostly $(\alpha4)_2(\beta2XFP)_3$ have higher FRET efficiency than the cells expressing mostly $(\alpha4)_3(\beta2XFP)_2$ receptors, as predicted (Figure 2C, D). These conclusions are supported by a rather different type of fluorescence analysis, FIR (Zheng and Zagotta, 2004) (Supplementary) Figure 7. Table 1 summarizes how these results generally agree with the previously reported shifts observed by metabolic labeling with [^{35}S] methionine, and biphasic dose response curves.

Importantly, one can perform these fluorescence-based measurements using live cultures. Pixel-by-pixel sensitized emission measurements are conducted with minimal destruction of the fluorophores (Figure 5 and 6), in principal allowing repeated observations on a single cell. Using this information, one can determine the changes in the subunit stoichiometry due to ADNFLE mutations, due to environmental conditions such as incubation temperature, or due to chaperoning by ligand (nicotine) interaction. The addictive properties of nicotine are thought to depend partially on these ligand-induced changes in subunit number and stoichiometry. The (inadvertent) therapeutic effects of smoking in ADNFLE (analyzed in this paper), and perhaps the inverse correlation between smoking and Parkinson's disease, arise from similar changes (Nashmi et al.,

Molecular Pharmacology Fast Forward. Published on February 23, 2009 as DOI: 10.1124/mol.108.054494
This article has not been copyedited and formatted. The final version may differ from this version.

2007). Therefore, we expect that fluorescence of nAChR subunits will become a useful procedure for drug discovery.

Molecular Pharmacology Fast Forward. Published on February 23, 2009 as DOI: 10.1124/mol.108.054494
This article has not been copyedited and formatted. The final version may differ from this version.

Acknowledgments

We thank Princess Imoukhuede, Rigo Pantoja, Rahul Srinivasan, Larry Wade, and Ben Corry (University of Western Australia) for discussion and Jeff Larsen (Nikon) for much technical help.

Requests for Reprints: Henry A. Lester, California Institute of Technology, Division of Biology M/C 156-29, Pasadena, CA 91107. E-mail: lester@caltech.edu

References

Balch WE, Morimoto RI, Dillin A and Kelly JW (2008) Adapting proteostasis for disease intervention. *Science* **319**(5865):916-919.

Benowitz NL, Kuyt F and Jacob P, 3rd (1982) Circadian blood nicotine concentrations during cigarette smoking. *Clin Pharmacol Ther* **32**(6):758-764.

Bertrand D, Picard F, Le Hellard S, Weiland S, Favre I, Phillips H, Bertrand S, Berkovic SF, Malafosse A and Mulley J (2002) How mutations in the nAChRs can cause ADNFLE epilepsy. *Epilepsia* **43 Suppl 5**:112-122.

Briggs CA, Gubbins EJ, Marks MJ, Putman CB, Thimmapaya R, Meyer MD and Surowy CS (2006) Untranslated region-dependent exclusive expression of high-sensitivity subforms of α4β2 and α3β2 nicotinic acetylcholine receptors. *Mol Pharmacol* **70**(1):227-240.

Brodtkorb E and Picard F (2006) Tobacco habits modulate autosomal dominant nocturnal frontal lobe epilepsy. *Epilepsy Behav* **9**(3):515-520.

Buisson B and Bertrand D (2001) Chronic exposure to nicotine upregulates the human α4β2 nicotinic acetylcholine receptor function. *J Neurosci* **21**(6):1819-1829.

Combi R, Dalpra L, Tenchini ML and Ferini-Strambi L (2004) Autosomal dominant nocturnal frontal lobe epilepsy--a critical overview. *J Neurol* **251**(8):923-934.

Corry B and Jayatilaka D (2008) Simulation of structure, orientation, and energy transfer between AlexaFluor molecules attached to MscL. *Biophys J* **95**(6):2711-2721.

Corry B, Jayatilaka D, Martinac B and Rigby P (2006) Determination of the orientational distribution and orientation factor for transfer between membrane-bound fluorophores using a confocal microscope. *Biophys J* **91**(3):1032-1045.

Corry B, Jayatilaka D and Rigby P (2005) A flexible approach to the calculation of resonance energy transfer efficiency between multiple donors and acceptors in complex geometries. *Biophys J* **89**(6):3822-3836.

Derry CP, Davey M, Johns M, Kron K, Glencross D, Marini C, Scheffer IE and Berkovic SF (2006) Distinguishing sleep disorders from seizures: diagnosing bumps in the night. *Arch Neurol* **63**(5):705-709.

Drenan RM, Nashmi R, Imoukhuede PI, Just H, McKinney S and Lester HA (2008) Subcellular Trafficking, Pentameric Assembly and Subunit Stoichiometry of Neuronal Nicotinic ACh Receptors Containing Fluorescently-Labeled α6 and β3 Subunits. *Mol Pharmacol* **73**:27-41.

Elangovan M, Wallrabe H, Chen Y, Day RN, Barroso M and Periasamy A (2003) Characterization of one- and two-photon excitation fluorescence resonance energy transfer microscopy. *Methods* **29**(1):58-73.

Feige JN, Sage D, Wahli W, Desvergne B and Gelman L (2005) PixFRET, an ImageJ plug-in for FRET calculation that can accommodate variations in spectral bleed-throughs. *Microsc Res Tech* **68**(1):51-58.

Figl A, Viseshakul N, Shafaee N, Forsayeth J and Cohen BN (1998) Two mutations linked to nocturnal frontal lobe epilepsy cause use-dependent potentiation of the nicotinic ACh response. *J Physiol (Lond)* **513**(Pt 3):655-670.

Fonck C, Cohen BN, Nashmi R, Whiteaker P, Wagenaar D, Rodrigues-Pinguet N, Deshpande P, Kwoh S, Munoz J, Labarca C, Collins AC, Marks M and Lester HA (2005) Novel seizure phenotype and sleep disruptions in knock-in mice with hypersensitive α4 nicotinic receptors. *J Neurosci* **25**:11396-113411.

Fonck C, Nashmi R, Deshpande P, Damaj M, Marks M, Riedel A, Schwarz J, Collins AC, Labarca C and Lester HA (2003) Increased sensitivity to agonist-induced seizures, Straub tail, and

hippocampal theta rhythm in knock-in mice carrying hypersensitive α4 nicotinic receptors. *J Neurosci* **23**:2582-2590.

Herman ST, Walczak TS and Bazil CW (2001) Distribution of partial seizures during the sleep-wake cycle: differences by seizure onset site. *Neurology* **56**(11):1453-1459.

Imoukhuede PI, Moss FJ, Michael DJ, Chow RH and Lester HA (2009) Ezrin mediates tethering of the γ-aminobutyric acid transporter GAT1 to actin filaments via a C-terminal PDZ-interacting domain. *Biophys J* **96**(7):in press.

Khakh BS, Fisher JA, Nashmi R, Bowser DN and Lester HA (2005) An angstrom scale interaction between plasma membrane ATP-gated P2X2 and α4β2 nicotinic channels measured with FRET and TIRF microscopy. *J Neurosci* **25**:6911-6920.

Klaassen A, Glykys J, Maguire J, Labarca C, Mody I and Boulter J (2006) Seizures and enhanced cortical GABAergic inhibition in two mouse models of human autosomal dominant nocturnal frontal lobe epilepsy. *Proc Natl Acad Sci U S A* **103**(50):19152-19157.

Kuryatov A, Luo J, Cooper J and Lindstrom J (2005) Nicotine acts as a pharmacological chaperone to up-regulate human α4β2 acetylcholine receptors. *Mol Pharmacol* **68**(6):1839-1851.

Kuryatov A, Onksen J and Lindstrom J (2008) Roles of accessory subunits in α4β2α5 nicotinic receptors. *Mol Pharmacol* **74**(1):132-143.

Mansvelder HD and McGehee DS (2000) Long-term potentiation of excitatory inputs to brain reward areas by nicotine. *Neuron* **27**(2):349-357.

Moroni M, Zwart R, Sher E, Cassels BK and Bermudez I (2006) α4β2 nicotinic receptors with high and low acetylcholine sensitivity: pharmacology, stoichiometry, and sensitivity to long-term exposure to nicotine. *Mol Pharmacol* **70**(2):755-768.

Nashmi R, Dickinson ME, McKinney S, Jareb M, Labarca C, Fraser SE and Lester HA (2003) Assembly of α4β2 nicotinic acetylcholine receptors assessed with functional fluorescently

labeled subunits: effects of localization, trafficking, and nicotine-induced upregulation in clonal mammalian cells and in cultured midbrain neurons. *J Neurosci* **23**(37):11554-11567.

Nashmi R and Lester HA (2007) Cell autonomy, receptor autonomy, and thermodynamics in nicotine receptor up-regulation. *Biochem Pharmacol* **74**(8):1145-1154.

Nashmi R, Xiao C, Deshpande P, McKinney S, Grady SR, Whiteaker P, Huang Q, McClure-Begley T, Lindstrom JM, Labarca C, Collins AC, Marks MJ and Lester HA (2007) Chronic nicotine cell specifically upregulates functional α4* nicotinic receptors: basis for both tolerance in midbrain and enhanced long-term potentiation in perforant path. *J Neurosci* **27**(31):8202-8218.

Nelson ME, Kuryatov A, Choi CH, Zhou Y and Lindstrom J (2003) Alternate stoichiometries of α4β2 nicotinic acetylcholine receptors. *Mol Pharmacol* **63**(2):332-341.

Oldani A, Zucconi M, Asselta R, Modugno M, Bonati MT, Dalpra L, Malcovati M, Tenchini ML, Smirne S and Ferini-Strambi L (1998) Autosomal dominant nocturnal frontal lobe epilepsy. A video-polysomnographic and genetic appraisal of 40 patients and delineation of the epileptic syndrome. *Brain* **121**:205-223.

Partridge JG, Apparsundaram S, Gerhardt GA, Ronesi J and Lovinger DM (2002) Nicotinic acetylcholine receptors interact with dopamine in induction of striatal long-term depression. *J Neurosci* **22**(7):2541-2549.

Provini F, Plazzi G, Tinuper P, Vandi S, Lugaresi E and Montagna P (1999) Nocturnal frontal lobe epilepsy. A clinical and polygraphic overview of 100 consecutive cases. *Brain* **122**:1017-1031.

Rodrigues-Pinguet N, Jia L, Li M, Figl A, Klaassen A, Truong A, Lester HA and Cohen BN (2003) Five ADNFLE mutations reduce the Ca^{2+} dependence of the α4β2 acetylcholine response. *J Physiol* **550**:11-26.

Molecular Pharmacology Fast Forward. Published on February 23, 2009 as DOI: 10.1124/mol.108.054494
This article has not been copyedited and formatted. The final version may differ from this version.

Rodrigues-Pinguet NO, Pinguet TJ, Figl A, Lester HA and Cohen BN (2005) Mutations linked to autosomal dominant nocturnal frontal lobe epilepsy affect allosteric Ca^{2+} activation of the $\alpha4\beta2$ nicotinic acetylcholine receptor. *Mol Pharmacol* **68**(2):487-501.

Ryvlin P, Rheims S and Risse G (2006) Nocturnal frontal lobe epilepsy. *Epilepsia* **47 Suppl 2**:83-86.

Sallette J, Pons S, Devillers-Thiery A, Soudant M, Prado de Carvalho L, Changeux JP and Corringer PJ (2005) Nicotine upregulates its own receptors through enhanced intracellular maturation. *Neuron* **46**(4):595-607.

Scheffer IE, Bhatia KP, Lopes-Cendes I, Fish DR, Marsden CD, Andermann E, Andermann F, Desbiens R, Keene D, Cendes F and et al. (1995) Autosomal dominant nocturnal frontal lobe epilepsy. A distinctive clinical disorder. *Brain* **118**:61-73.

Staruschenko A, Adams E, Booth RE and Stockand JD (2005) Epithelial Na^{+} channel subunit stoichiometry. *Biophys J* **88**(6):3966-3975.

Steinlein OK, Magnusson A, Stoodt J, Bertrand S, Weiland S, Berkovic SF, Nakken KO, Propping P and Bertrand D (1997) An insertion mutation of the CHRNA4 gene in a family with autosomal dominant nocturnal frontal lobe epilepsy. *Hum Mol Genet* **6**(6):943-947.

Teper Y, Whyte D, Cahir E, Lester HA, Grady SR, Marks MJ, Cohen BN, Fonck C, McClure-Begley T, McIntosh JM, Labarca C, Lawrence A, Chen F, Gantois I, Davies PJ, Petrou S, Murphy M, Waddington J, Horne MK, Berkovic SF and Drago J (2007) Nicotine-induced dystonic arousal complex in a mouse line harboring a human autosomal dominant nocturnal frontal lobe epilepsy mutation. *J Neurosci* **27**:10128-10142.

Vallejo YF, Buisson B, Bertrand D and Green WN (2005) Chronic nicotine exposure upregulates nicotinic receptors by a novel mechanism. *J Neurosci* **25**(23):5563-5572.

Willoughby JO, Pope KJ and Eaton V (2003) Nicotine as an antiepileptic agent in ADNFLE: an N-of-one study. *Epilepsia* **44**(9):1238-1240.

Wimmer VC, Lester HA and Petrou S (2008) Ion channel mutations in familial epilepsy, in *Encyclopedia of Epilepsy Research* (Schwartzkroin PA ed), Elsevier, Oxford.

Wiseman RL, Powers ET, Buxbaum JN, Kelly JW and Balch WE (2007) An adaptable standard for protein export from the endoplasmic reticulum. *Cell* **131**(4):809-821.

Wong JY, Ross SA, McColl C, Massalas JS, Powney E, Finkelstein DI, Clark M, Horne MK, Berkovic SF and Drago J (2002) Proconvulsant-induced seizures in α4 nicotinic acetylcholine receptor subunit knockout mice. *Neuropharmacology* **43**(1):55-64.

Zheng J and Zagotta WN (2004) Stoichiometry and assembly of olfactory cyclic nucleotide-gated channels. *Neuron* **42**(3):411-421.

Zwart R, Broad LM, Xi Q, Lee M, Moroni M, Bermudez I and Sher E (2006) 5-I A-85380 and TC-2559 differentially activate heterologously expressed α4αβ2 nicotinic receptors. *Eur J Pharmacol* **539**(1-2):10-17.

Molecular Pharmacology Fast Forward. Published on February 23, 2009 as DOI: 10.1124/mol.108.054494
This article has not been copyedited and formatted. The final version may differ from this version.

Footnote

This work was supported by grants from the National institutes of Health [NS11756] and from Targacept, Inc. Cagdas D. Son and Fraser J. Moss were supported by fellowships from Philip Morris USA/International and from the American Heart Association, respectively.

Molecular Pharmacology Fast Forward. Published on February 23, 2009 as DOI: 10.1124/mol.108.054494
This article has not been copyedited and formatted. The final version may differ from this version.

Legends for Figures

Figure 1. Assumptions and calculations underlying the FRET analyses.

A, In a pentamer, there are two possible distances between fluorophores: "*a*" the side length of the pentagon, and "*b*" the diagonal between non-adjacent subunits. See Appendix, Equation 4.

B, Fractional prevalence of various arrangements when two or three tagged subunits are present in pentameric nAChRs. FRET efficiencies E, E1, E2, E3, E4 are given in Appendix, Equations 5-9 (Corry et al., 2005).

C, Theoretical FRET efficiency versus distance *a* between adjacent fluorophores in α4 subunits, for α4β2 receptor populations containing several overall stoichiometric ratios of α4 to β2. Calculations use Appendix Eqs. 7, 8, 9, and 10 plus the known statistical factors (Corry et al., 2005). For the CFP-YFP pair, R_0 = 50 Å. Note that X-axis is defined by the length of a side, rather than the definition given by Figures 10 and 12 of Corry et al (2005).

D, Dashed line, calculated FRET efficiency for fluorescent α4 subunits, versus percentage of receptors with $(\alpha4)_3(\beta2)_2$ stoichiometry (the balance of pentamers would be $(\alpha4)_2(\beta2)_3$). The solid line provides the complementary calculation for receptors with fluorescent β2 subunits. The calculations assume that the separation between adjacent fluorophores, *a* = 52 Å (vertical line in C).

Figure 2. Spectral images acquired before and after YFP bleaching were unmixed in order to calculate percent increase and decrease in CFP and YFP fluorescence intensities, respectively.

A, Representative unmixed images of a single N2a cell expressing 1:1 transfection ratio of α4XFP:β2 cDNAs before and after photobleaching of the YFP fluorophore.

B, Time course of changes in CFP and YFP fluorescence intensity.

Molecular Pharmacology Fast Forward. Published on February 23, 2009 as DOI: 10.1124/mol.108.054494
This article has not been copyedited and formatted. The final version may differ from this version.

C, Scatter plot of CFP intensity increase vs YFP intensity decrease. This is extrapolated to 100% on the X-axis, for the calculation of FRET efficiency (Equation 1).

D, E, FRET efficiencies measured for transfections with forced stoichiometries. **D**, Increased β2 cDNA concentration during transfection with the α4XFP results in a decrease in % FRET efficiency. **E,** Increased β2XFP cDNA concentration during transfection with α4 results in an increase in % FRET efficiency.

Figure 3. ADNFLE mutations bias the α4β2 receptor population toward the $(\alpha4)_3(\beta2)_2$ stoichiometry.

A and **B** show FRET efficiency values measured by the DRAP method for five non-fluorescent ADNFLE mutant subunits transfected into N2a cells with the fluorescent WT complementary subunits (α4XFP or β2XFP, where XFP denotes a 1:1 mixture of the CFP and YFP subunits). **A,** 1:4 cDNA ratio of α4 to β2 subunits was transfected. **B,** 1:1 cDNA ratio of α4 to β2 subunits was transfected.

C and **D** show FRET efficiency values measured by the DRAP method for five fluorescent ADNFLE mutant subunits (α4XFP or β2XFP, where XFP denotes a 1:1 mixture of the CFP and YFP ADNFLE subunits), transfected into N2a cells with the non-fluorescent WT complementary subunits. **C,** 1:4 cDNA ratio of α4 to β2 subunits was transfected. **D,** 1:1 cDNA ratio of α4 to β2 subunits was transfected.

Data show mean ± S. E. M. (# of cells given in each bar). Significance was tested with unpaired two tailed t-Test, * indicates $p \leq 0.05$, and ** indicates $p \leq 0.01$.

Figure 4. Incubation in nicotine shifts both the WT receptor (**A)** and an ADNFLE receptor (**B)** toward the $(\alpha4)_2(\beta2)_3$ stoichiometry. FRET efficiency values were measured by the DRAP method.

Molecular Pharmacology Fast Forward. Published on February 23, 2009 as DOI: 10.1124/mol.108.054494
This article has not been copyedited and formatted. The final version may differ from this version.

A, FRET efficiency measured for N2a cells transfected with 1:1 cDNA ratio of α4XFP:β2 or α4:β2XFP in the presence or absence of nicotine.

B, FRET efficiency calculations for the N2a cells transfected with 1:1 cDNA ratio of α4:β2 (V287L)XFP or α4XFP:β2(V287L) in the presence or absence of nicotine.

Data show mean ± S. E. M. (# of cells given in each bar).

Figure 5. Representative pixel-resolved sensitized emission FRET images for various conditions. Column 1 displays unmixed cell images in the CFP channel after 439 nm excitation; Column 2 displays unmixed cell images in the YFP channel after 514 nm excitation; Column 3 displays the % FRET efficiency images. Nicotine was present at 1 μM for 48 h where indicated.

Row A, WT α4 subunit plus β2XFP

Rows B and **C**, WT α4 subunit plus β2(V287L)XFP. **B,** control incubation; **C,** incubation in nicotine.

Row D, α4XFP plus WT β2.

Rows E and **F**, α4XFP subunit plus β2V287L. **E,** control incubation; **F,** incubation in nicotine.

G, Average FRET efficiencies. Each column gives average over all pixels for 20-25 cells in each case. The S. E. M. is smaller than the width of the line in all cases.

Data show mean ± S. E. M. (# of cells given in each bar). The S. E. M. (approximately the size of the lines delimiting the boxes) are smaller than in DRAP experiments, because S. E. M. is calculated on the basis of pixel numbers.

Figure 6. Nicotine shifts the population of α4 S248F ADNFLE receptors toward the $(\alpha4)_2(\beta2)_3$ stoichiometry. Representative pixel-resolved sensitized emission % FRET images. **A**, saline for

Molecular Pharmacology Fast Forward. Published on February 23, 2009 as DOI: 10.1124/mol.108.054494
This article has not been copyedited and formatted. The final version may differ from this version.

48 h; **B**, nicotine, 1 μM, 48 h. **C**, the graph shows data for a total of ~ 5 x 10^6 pixels from 37 and 40 cells, respectively. Data show mean ± S. E. M.. The S. E. M. is approximately the size of the lines delimiting the boxes.

Molecular Pharmacology Fast Forward. Published on February 23, 2009 as DOI: 10.1124/mol.108.054494
This article has not been copyedited and formatted. The final version may differ from this version.

Table

Table 1. Percent of $(\alpha4)_3(\beta2)_2$ for WT nAChRs observed under various conditions in this study and a previous study.

cDNAs	α4 : β2					
Ratios	4:1	1:1	1:4	1:9	1:1	
Other					Nicotine	30 °C
FIR	100	83	45	13	73	N. D.
FRET	94 ± 7	75 ± 3.5	52 ± 3	28± 3	61 ± 6	55 ± 6
Reported*	N. R.	82	43 ± 4	N. R.	68 ± 5	67 ± 6

FIR and FRET efficiency measurements were used to determine the subunit stoichiometry from cells transfected with various ratios of subunit cDNA and exposed to nicotine or low incubation temperatures. FRET measurements for WT subunits are derived from the experiment of Figure 2C, D; FIR measurements from the experiment of (Supplementary) Figure 7. Data for incubation at 30° C are not shown. Results are compared to reported values. N.R. = not reported, N.D. = not determined in the present experiments. * (Nelson et al., 2003)

Molecular Pharmacology Fast Forward. Published on February 23, 2009 as DOI: 10.1124/mol.108.054494
This article has not been copyedited and formatted. The final version may differ from this version.

Figure 1

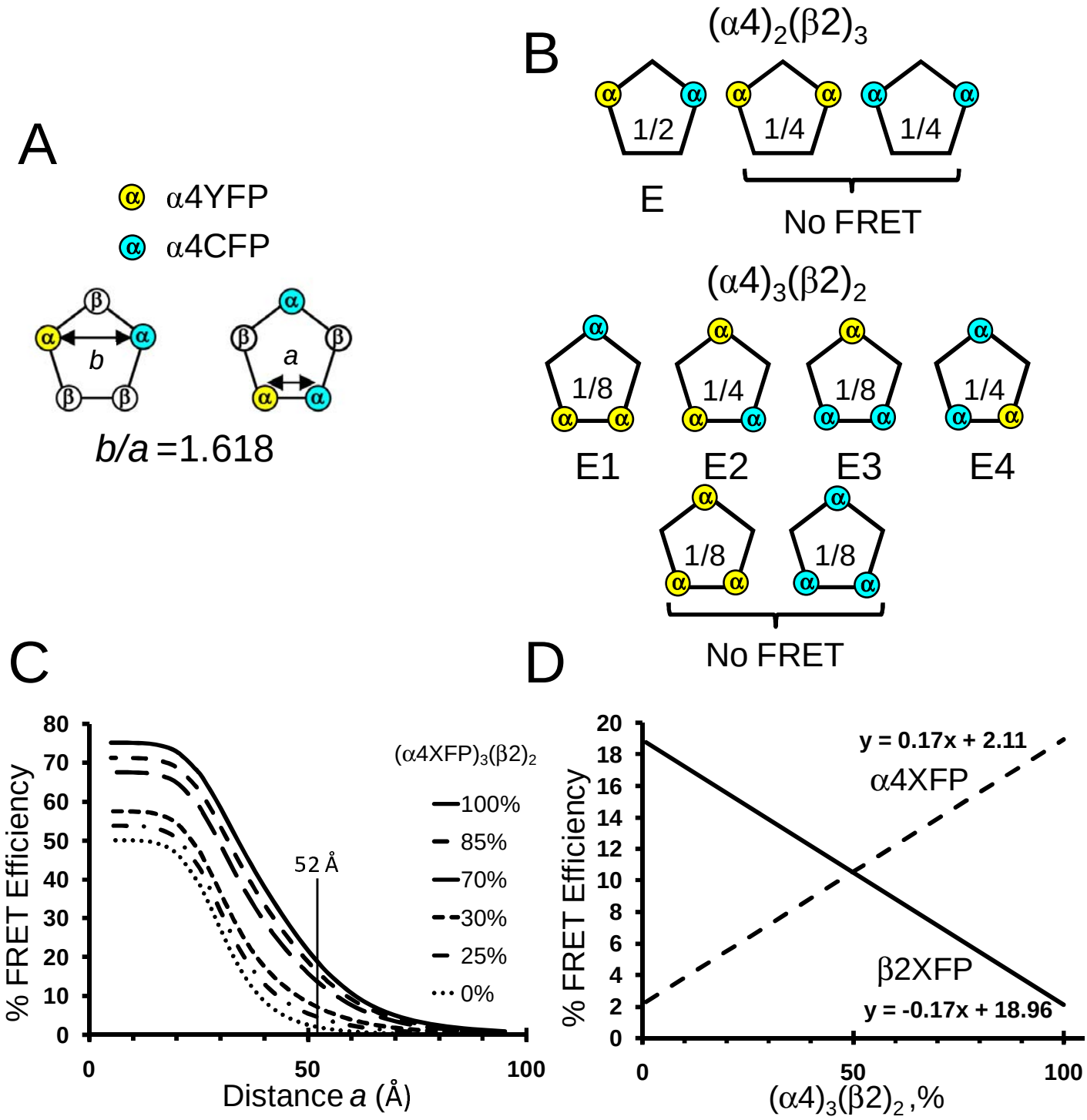

Molecular Pharmacology Fast Forward. Published on February 23, 2009 as DOI: 10.1124/mol.108.054494
This article has not been copyedited and formatted. The final version may differ from this version.

Figure 2

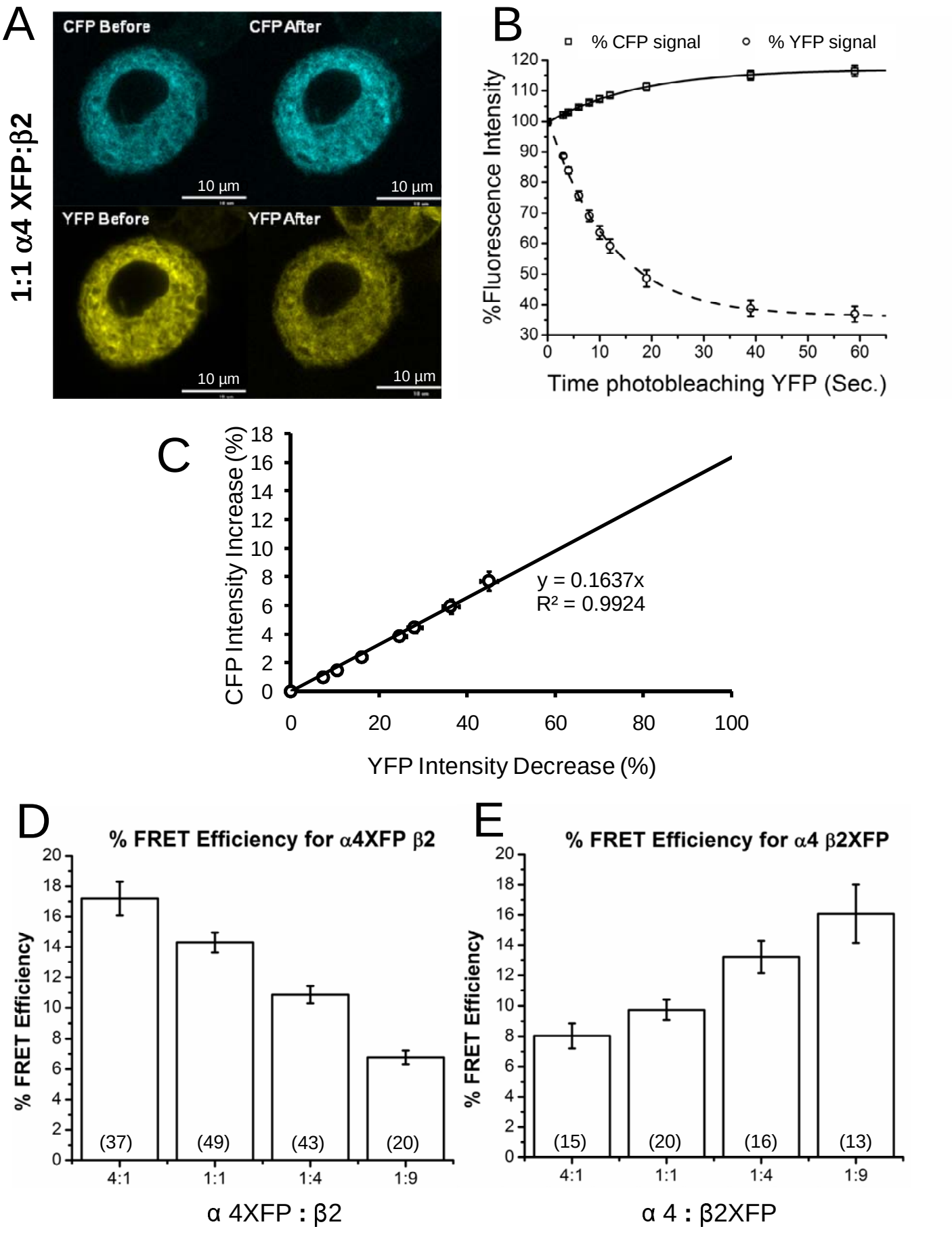

Molecular Pharmacology Fast Forward. Published on February 23, 2009 as DOI: 10.1124/mol.108.054494
This article has not been copyedited and formatted. The final version may differ from this version.

Figure 3

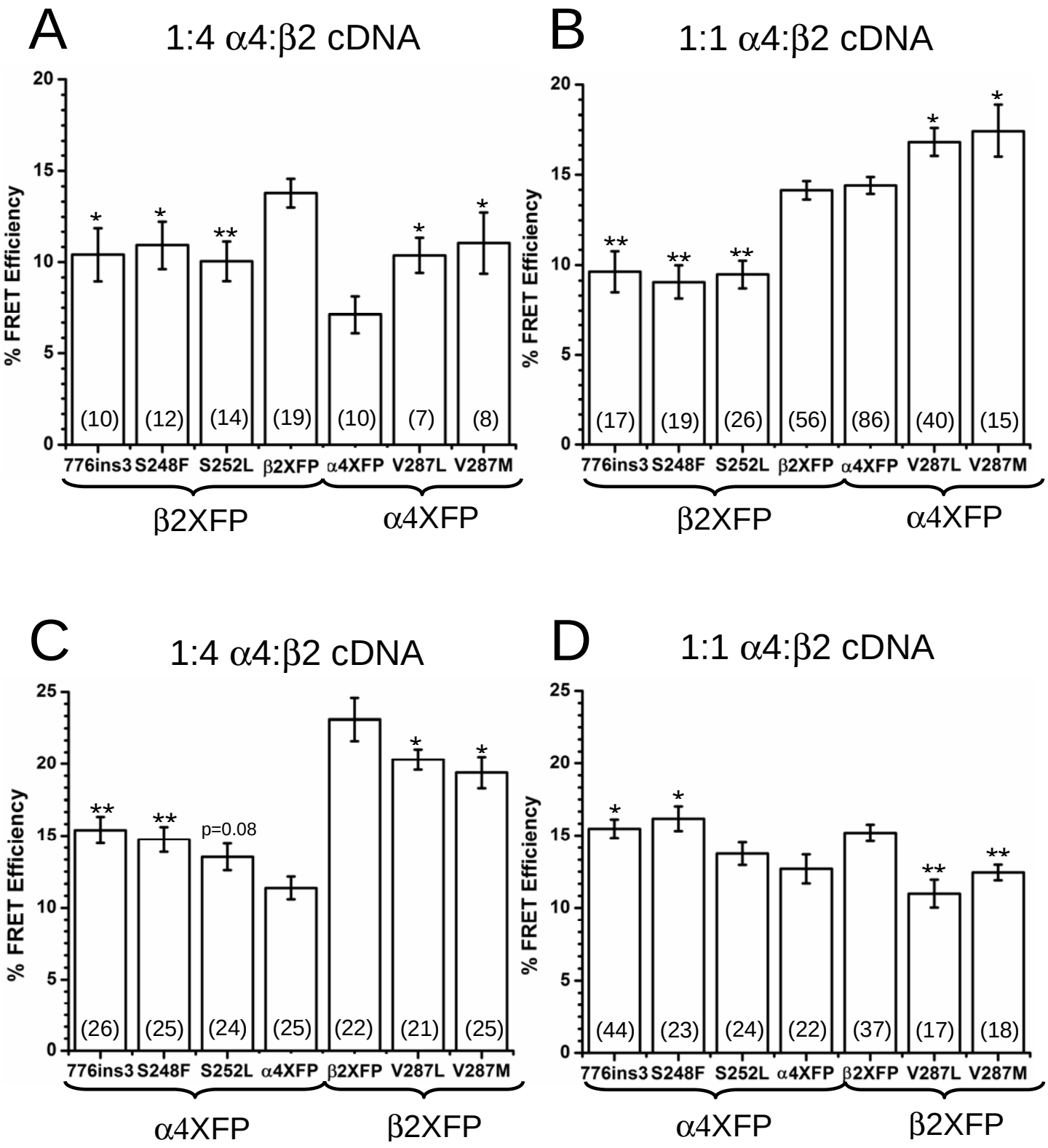

Molecular Pharmacology Fast Forward. Published on February 23, 2009 as DOI: 10.1124/mol.108.054494
This article has not been copyedited and formatted. The final version may differ from this version.

Figure 4

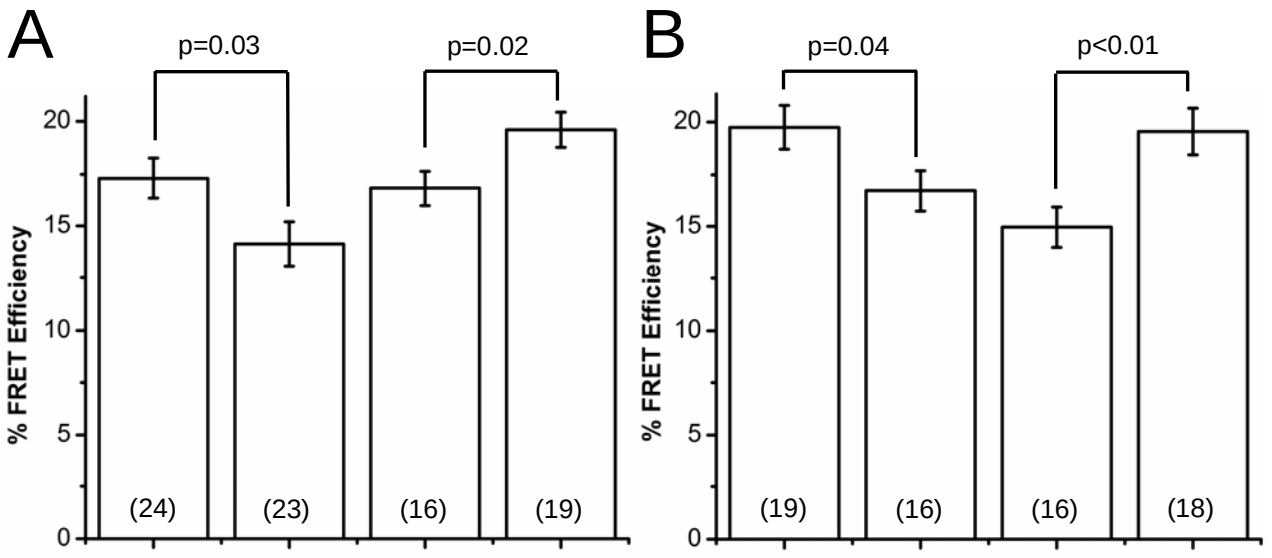

α4	XFP	XFP	WT	WT
β2	WT	WT	XFP	XFP
Nicotine	-	+	-	+

XFP	XFP	WT	WT
VL	VL	VL,XFP	VL,XFP
-	+	-	+

Molecular Pharmacology Fast Forward. Published on February 23, 2009 as DOI: 10.1124/mol.108.054494
This article has not been copyedited and formatted. The final version may differ from this version.

Figure 5

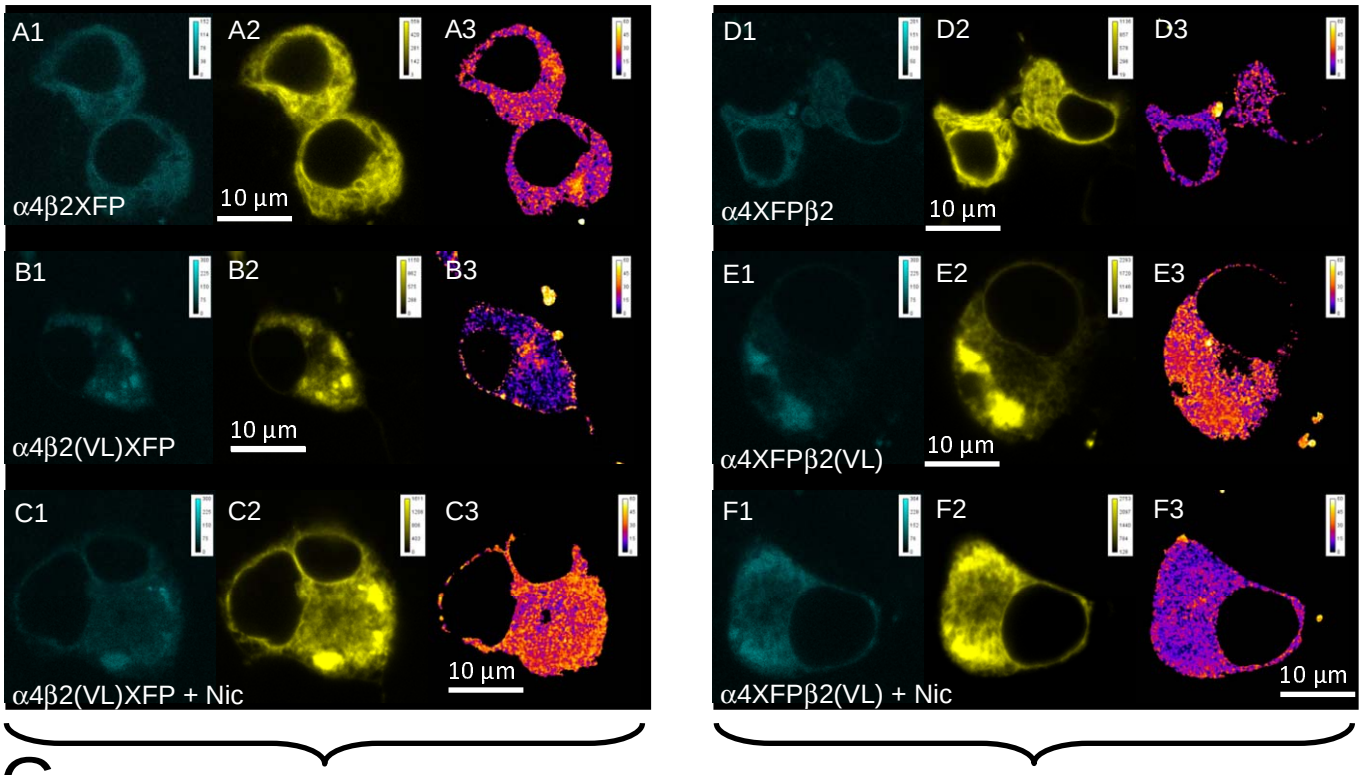

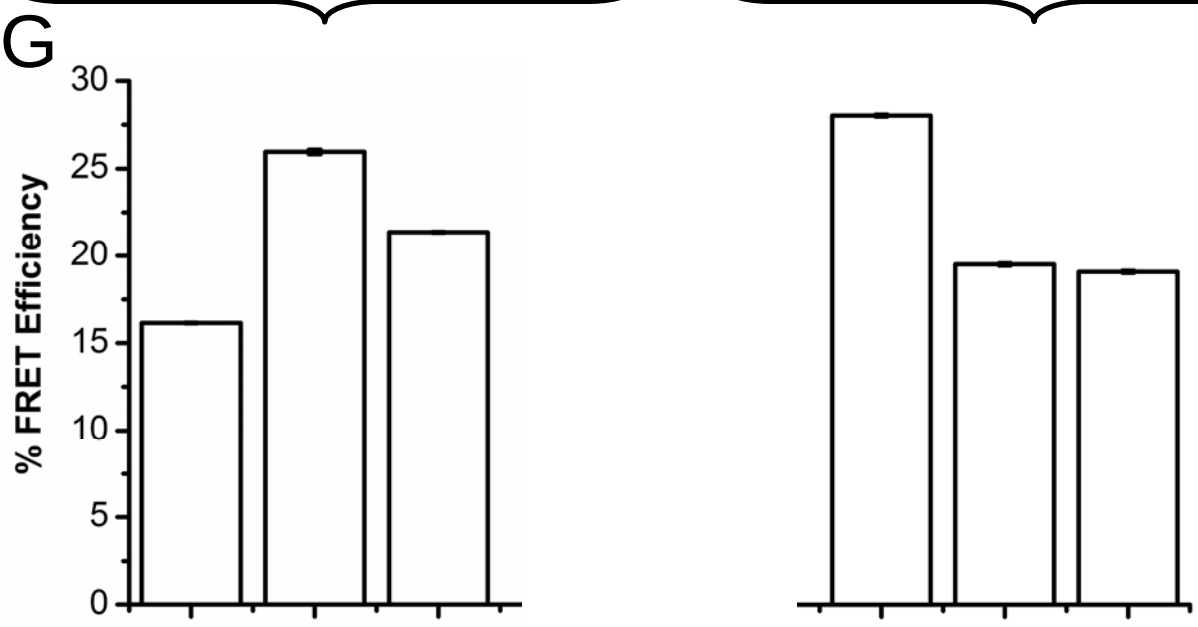

α4	WT	WT	WT
β2	VL,XFP	VL,XFP	XFP
Nicotine	-	+	-

XFP	XFP	XFP
VL	VL	WT
-	+	-

Molecular Pharmacology Fast Forward. Published on February 23, 2009 as DOI: 10.1124/mol.108.054494
This article has not been copyedited and formatted. The final version may differ from this version.

Figure 6

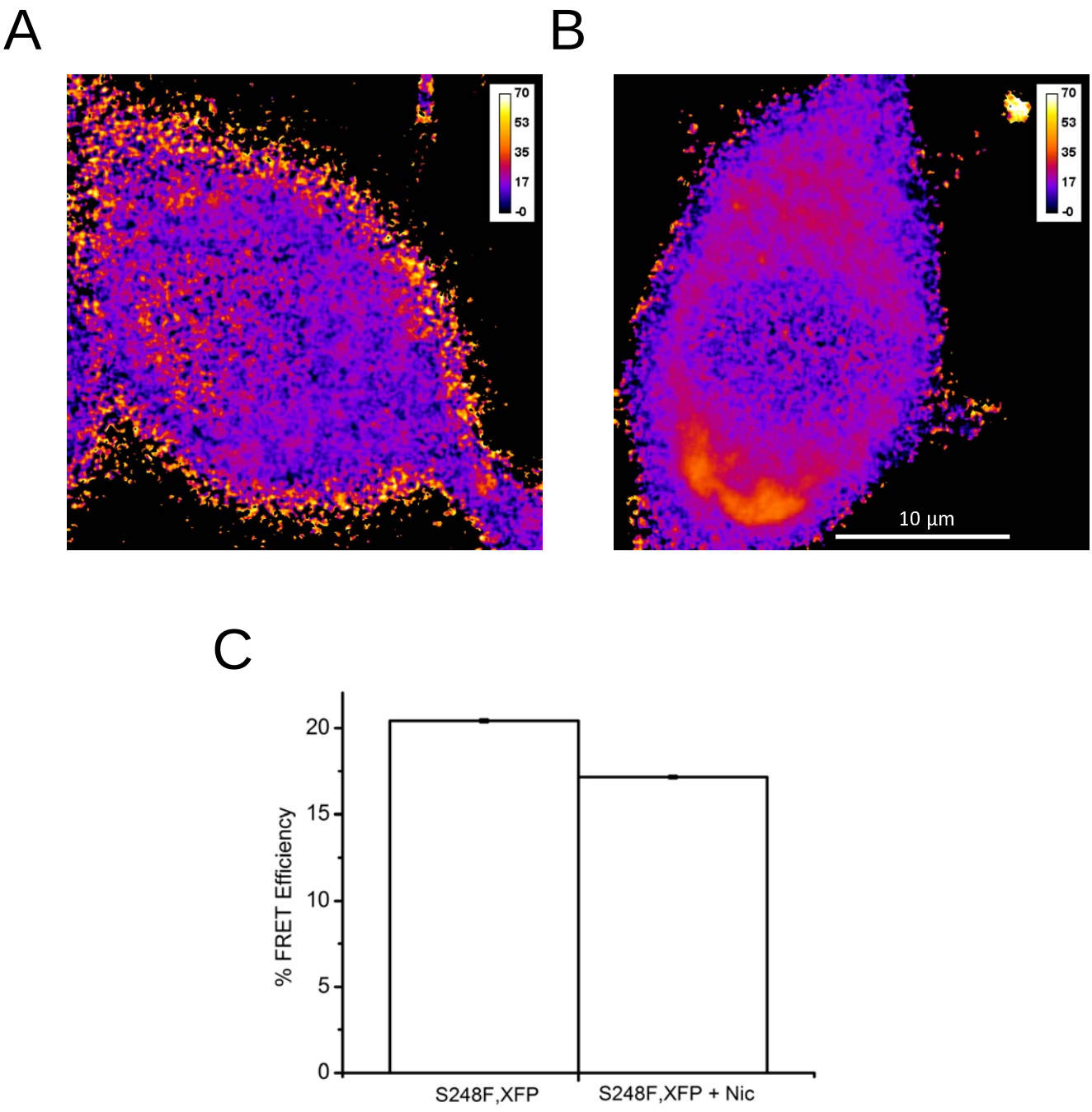

Molecular Pharmacology Fast Forward. Published on February 23, 2009 as DOI: 10.1124/mol.108.054494
This article has not been copyedited and formatted. The final version may differ from this version.

Appendix

This Appendix presents the theory of FRET measurements to determine subunit stoichiometry. The analysis uses several simplifying geometric assumptions. (1) In a functional α4β2 receptor, there are at least two agonist binding sites at the α-β subunit interfaces (these are polarized, requiring particular faces of each subunit; see assumption 2 below). Therefore, in the $(\alpha4)_2(\beta2)_3$ stoichiometry, the two α4 subunits are non-adjacent; and in the $(\alpha4)_3(\beta2)_2$ stoichiometry, the two β2 subunits are non-adjacent. (2) In the diagrams of Figure 1A, B the receptor is viewed from the extracellular faces, so that the β subunit is adjacent, in the clockwise direction, to the α subunit. (3) Although the intracellular domain of the α4 subunit has roughly twice as many amino acids as that of the β2 subunit, the fluorophores are positioned in an equilateral pentagonal structure. (4) All α4 subunits are radially equivalent; and all β2 subunits are radially equivalent. (5) Because YFP and CFP differ by only 9 amino acids, YFP-tagged and CFP-tagged subunits are synthesized with equal efficiency and assemble randomly within receptor pentamers. The expected results are rather insensitive to departures from this assumption by even two-fold. (6), Again because YFP and CFP differ only subtly, the structure of an α4CFP subunit is the same as α4YFP; also a β2CFP subunit has the same structure as a β2YFP subunit. (7) In a rigorous analysis, the dipole orientation factor κ^2 differs between adjacent and non-adjacent subunit pairs. Analysis shows that, in general, the ratio κ^2 (non-adjacent subunits) / κ^2 (adjacent subunits) lies between 1 and 2; a full prediction requires knowledge of the dipole orientation, which we do not know (Corry et al., 2006). We assume that this ratio always equals 1.

In such a pentameric receptor, there are two possible distances between fluorophores: *a*, the side length between adjacent subunits; and *b*, the diagonal between non-adjacent subunits (Figure 1A). These are given by:

Molecular Pharmacology Fast Forward. Published on February 23, 2009 as DOI: 10.1124/mol.108.054494
This article has not been copyedited and formatted. The final version may differ from this version.

$$b/a = \left(1+\sqrt{5}/2\right) = 1.618 \qquad \text{(Equation 4)}$$

Thus the efficiencies of energy transfer within an isolated pentameric receptor can be calculated analytically depending on the position of the donor and the acceptor. Most measurements in this study use the simple case in which the fluorophores are present in all α4 subunits, but none of the β2 subunits, or vice-versa. To simplify the terminology, we explicitly analyze the case for fluorescent α4 subunits; the results apply, of course, to the fluorescent β2 case as well.

For the $(\alpha4)_2(\beta2)_3$ stoichiometry, the fluorophore separation is the non-adjacent value, *b*. Therefore the FRET efficiency is

$$E_b = \left(\frac{\left(R_0/b\right)^6}{1+\left(R_0/b\right)^6} \right); \qquad \text{(Equation 5)}$$

and the statistical factors are rather simple: 50% of the molecules have heterogeneous fluorophores and therefore display FRET (our methods do not determine homo-FRET) (Figure 1B).

The situation is more complex for the $(\alpha4)_3(\beta2)_2$ pentamer (Figure 1B). For instance, the FRET efficiency for one donor, non-adjacent to two acceptors, is

$$E_1 = \left(\frac{2\left(R_0/b\right)^6}{1+2\left(R_0/b\right)^6} \right); \qquad \text{(Equation 6)}$$

for one donor, adjacent and non-adjacent to two acceptors, *E* is

$$E_2 = \left(\frac{R_0^6\left(\frac{1}{a^6}+\frac{1}{b^6}\right)}{1+R_0^6\left(\frac{1}{a^6}+\frac{1}{b^6}\right)} \right); \qquad \text{(Equation 7)}$$

Molecular Pharmacology Fast Forward. Published on February 23, 2009 as DOI: 10.1124/mol.108.054494
This article has not been copyedited and formatted. The final version may differ from this version.

for two donors, both non-adjacent to a single acceptor, E is simply

$$E_3 = E_b. \qquad \text{(Equation 8)}$$

For two donors, one adjacent and the other non-adjacent to a single acceptor,

$$E_4 = \frac{1}{2}\left(\frac{\left(\frac{R_0}{a}\right)^6}{1+\left(\frac{R_0}{a}\right)^6} + \frac{\left(\frac{R_0}{b}\right)^6}{1+\left(\frac{R_0}{b}\right)^6} \right). \qquad \text{(Equation 9)}$$

The total FRET efficiency is now the weighted sum of E for a particular configuration, times the probability that the configuration occurs. These statistical factors are given in Figure 1B (Corry et al., 2005).

These calculations lead to an expected series of FRET efficiencies as a function of the distance *a* between adjacent fluorophores (Figure 1C). Note that the FRET efficiency does not approach 1 as *a* approaches 0, because in some pentamers, all tagged subunits carry either donors or acceptors, in which case our measurement cannot detect FRET. Because 25% of the assembled receptors are composed of three tagged subunits and 50% of the receptors carrying two tagged subunits lack FRET partners, the FRET efficiency curves in Figure 1C intersect the y-axis between 75% and 50%.

The final step in the theoretical analysis (Figure 1D) is to assume a reasonable value for the distance *a* between adjacent fluorophores. In the absence of structural data for the intracellular loop of any Cys-loop receptor, this must be a guess. We assume a value of *a* = 52 Å, which is also consistent with structural studies of the neuromuscular receptor (Unwin, 2005). However any distance within ~40 Å and ~ 60 Å would generate the same conclusion: FRET efficiencies are quite

Molecular Pharmacology Fast Forward. Published on February 23, 2009 as DOI: 10.1124/mol.108.054494
This article has not been copyedited and formatted. The final version may differ from this version.

measureable (10% -40%) if all the pentamers have the $(\alpha4)_3(\beta2)_2$ stoichiometry. The solid line in Figure 1D shows that, as the percentage of $(\alpha4)_3(\beta2)_2$ decreases to zero (with a complementary increase of $(\alpha4)_2(\beta2)_3$), the theoretical FRET efficiency drops by ~10 fold.

For any chosen value of *a*, the theoretical FRET efficiency depends linearly on the percentage of $(\alpha4)_3(\beta2)_2$ stoichiometry. For *a* = 45 Å, the maximum and minimum FRET values are 29.3% and 4.8%, respectively; for *a* = 60 Å, these extremes are 10.6% and 0.9%, respectively.

Supplementary Material

Methods

Supplementary Table 1

Primer Name	**Primer Sequence**
S248F Forw.	5’ GCATC**TTC**GTGCTGCTTTCTCTCACCGTCTTCCTGCTGC 3’
S248F Rev.	5’ GCAC**CGA**GATGCACAGCGTGACCTTCTCGCCGCACTCC 3’
S252L Forw.	5’ GCTT**TTG**CTCACCGTCTTCCTGCTGCTCATCACCGAG 3’
S252L Rev.	5’ CGGTGAG**CAA**AAGCAGCACCGAGATGCACAGCGTGACC 3’
776ins3 Forw.	5’ GCTC**CTG**ATCACCGAGATCATCCCGTCCACCTCGCTGG 3’
776ins3 Rev.	5’ CGGTGAT**CAG**GAGCAGCAGGAAGACGGTGAGAGAAAGC 3’
V287L Forw.	5’ CCAAGATT**CTG**CCTCCCACCTCCCTCGACGTACCGCTGG 3’
V287L Rev.	5’ GGGAGG**CAG**AATCTTGGAGATGAGCAGCAGGAACACCG 3’
V287M Forw.	5’ CCAAGATT**ATG**CCTCCCACCTCCCTCGACGTACCGCTGG 3’
V287M Rev.	5’ GGGAGG**CAT**AATCTTGGAGATGAGCAGCAGGAACACCG 3’

Fluorescence Intensity Ratio Determinations of Subunit Stoichiometry

Fluorescence intensity ratio (FIR) analysis provides information to define the subunit stoichiometry of most heteromeric channel types. The method is based on fluorescently tagged subunits and was first reported (Zheng and Zagotta, 2004) to determine the subunit stoichiometry of olfactory cyclic nucleotide-gated channels. Our studies used the same YFP- and CFP-tagged α4 and β2 subunits used in the FRET studies. However, whereas the FRET studies employed 1:1 ratios of α4CFP:α4YFP (or the β2 equivalents), the FIR studies used two sets of cDNAs: (1) mixtures of α4CFP and β2YFP cDNAs, or (2) α4YFP and β2CFP cDNAs. Since the channel subunit and the fluorescent protein are covalently linked, the molar ratio between CFP and YFP molecules is the same as the molar ratio between the subunits in which they are inserted. To correct for different excitation laser intensities and different extinction coefficients and quantum yields of the fluorophores, a similar measurement was carried with set 1 and set 2. By comparing the two fluorescence ratios, we calculate the correction factor to account for the different intensities of the individual fluorophores and thereby calculate the ratio of subunits.

There are potential concerns with the FIR method. (a) FRET may occur between channel subunits. FIR assumes that fluorescence emission of CFP and YFP are independent. Considering the close proximity of channel subunits, this assumption is not true in most cases due to FRET between these fluorophores. (b) There may unassembled subunits present. (c) There may be degraded subunits, producing soluble CFP and YFP. Points (b) and (c) Would contribute to the fluorescence intensities measured, thus obscuring the subunit ratios calculated for the assembled channels. To overcome these complications, we used an analysis that we term “FRET-defined

FIR" to calculate the nAChR subunit stoichiometry. FRET-defined FIR assumes that FRET occurs only in fully assembled receptors, and that partially assembled receptors, free subunits, or free fluorophores do not contribute appreciable FRET.

For simplicity, we define α = α4 and β = β2. When CFP-tagged α subunits and YFP-tagged β subunits are co-expressed, the intensities of CFP and YFP can be calculated as $F_{CFP} = C_1[\alpha]$ and $F_{YFP} = C_2[\beta]$, where F_{CFP} and F_{YFP} are CFP and YFP intensities calculated by acceptor photobleaching. Thus, F_{CFP} corresponds to the dequenched CFP intensity when 100% of the acceptor molecules are bleached; this represents CFP carrying subunits participating in assembled pentamers with YFP containing subunits. Similarly F_{YFP} detected by exciting CFP at 439 nm and detecting the YFP emission due to FRET, arises from YFP containing subunits participating in assembled pentamers with CFP containing subunits. Both intensities were detected by spectral imaging and unmixed to eliminate background fluorescence and the overlap of emission spectra. The [α] and [β] are the number of αCFP and βYFP subunits. The constants C_1 and C_2 include the laser intensities, the system transfer function, the properties of the fluorophores, and other factors. But C_1 and C_2 are independent of the subunit (α vs β) hosting the fluorophore. The FIR

$$k_1 = \frac{F_{CFP}}{F_{YFP}} = C\frac{[\alpha]}{[\beta]}, \qquad \text{(Equation 10)}$$

where $C = C_1 / C_2$. Similarly, coexpressing αYFP and βCFP subunits yields an FIR

$$k_2 = \frac{F_{CFP}}{F_{YFP}} = C\frac{[\beta]}{[\alpha]}. \qquad \text{(Equation 11)}$$

Therefore, both the subunit ratio and the parameter *C* were determined using the following equations:

$$\frac{[\alpha]}{[\beta]} = \sqrt{k_1 / k_2}\,; \qquad \text{(Equation 12)}$$

$$C = \sqrt{k_1 k_2} \qquad \text{(Equation 13)}$$

Once *C* was experimentally determined for our optical system, we calculated k_1 and k_2 for any given subunit ratio. Comparison of the experimental data with these calculated values revealed the subunit stoichiometry under the experimental conditions.

(Supplementary) Figure 1. FIR measurements of the subunit ratio for α4β2 nAChRs. Scatter plot of the CFP intensity versus the YFP intensity (arbitrary calibrated units, (ACU)), measured from channels formed by α4YFP and β2CFP subunits (A, C and E), or α4CFP β2YFP (B, D and F). Each point is from an individual N2a cell. The dotted lines represent predicted fluorescence intensity ratio for 100% $(\alpha4)_2(\beta2)_3$ stoichiometry and the dashed lines represent 100% $(\alpha4)_3(\beta2)_2$ stoichiometry; the black lines are linear fits to each data set.

A, B, 1:1 ratio of α4:β2 cDNA.

C, D, 1:4 ratio of α4:β2 cDNA.

E, F, 1:9 ratio of α4:β2 cDNA.